Lasers and photodetectors for mid-infrared 2 – 3 μ m applications

Wen Lei and Chennupati Jagadish

Citation: Journal of Applied Physics **104**, 091101 (2008); doi: 10.1063/1.3002408
View online: http://dx.doi.org/10.1063/1.3002408
View Table of Contents: http://scitation.aip.org/content/aip/journal/jap/104/9?ver=pdfcov
Published by the AIP Publishing

APPLIED PHYSICS REVIEWS—FOCUSED REVIEW

Lasers and photodetectors for mid-infrared 2–3 μm applications

Wen Lei[a] and Chennupati Jagadish
Department of Electronic Materials Engineering, Research School of Physical Sciences and Engineering, Australian National University, Canberra, ACT 0200, Australia

(Received 5 May 2008; accepted 8 August 2008; published online 5 November 2008)

This paper presents an overview of the recent developments in III–V semiconductor lasers and detectors operating in the 2–3 μm wavelength range, which are highly desirable for various important applications, such as military, communications, molecular spectroscopy, biomedical surgery, and environmental protection. The lasers and detectors with different structure designs are discussed and compared. Advantages and disadvantages of each design are also discussed. Promising materials and structures to obtain high performance lasers and detectors operating in the 2–3 μm region are also suggested. © *2008 American Institute of Physics*.
[DOI: 10.1063/1.3002408]

TABLE OF CONTENTS

I. INTRODUCTION

Besides the mostly studied near-infrared (below 2 μm) and mid- and far-infrared (3–5) and 8–14 μm) optoelectronic devices, lasers and detectors operating in the mid-infrared (MIR) wavelength range (2–3 μm) at room temperature (RT) have attracted much attention recently. These MIR lasers and detectors are highly desirable for a variety of military, communications, molecular spectroscopy, biomedical surgery, environmental protection, and manufacturing industry applications. This is mainly due to the high transparency atmospheric window in the range of 2–2.3 μm and the strong absorption lines of many chemical molecules in the range of 2.3–3.0 μm, including all hydrocarbons.[1] A selected list of the molecule absorption lines and their corresponding applications are shown in Table I. For all these applications, semiconductor MIR lasers and detectors are the ideal candidates due to their intrinsic advantages of wide wavelength coverage, low cost, simplicity of operation and possibility of hybrid systems, and compact packages. Unfortunately, after the development of several decades, most currently used MIR semiconductor lasers and detectors still require low temperature operation because of some basic limitations, such as Auger nonradiative recombination, high thermal generation rate in the devices, etc. Also, for most of the applications the cryogenic coolers are not desirable because of their short lifetime and the added power consumption, weight, volume, and costs. Therefore, uncooled and multispectral semiconductor lasers and detectors operating continuously in the MIR 2–3 μm region are highly desirable.

In this paper, we will review the recent research progress of MIR III–V compound semiconductor lasers and detectors working in the 2–3 μm range. The performance of the lasers and detectors with different structure designs and differ-

TABLE I. Selected molecule absorption lines in the 2–3 μm region and their corresponding applications.

Molecules	Absorption lines (μm)	Applications
H_2O	2.3–2.8	Environmental monitoring/medical
CO	2.3	Environmental monitoring
NO	2.65	Environmental monitoring
CH_4	2.35	Environmental monitoring
Thyroxine	2.8	Medical

[a]Electronic mail: wen.lei@anu.edu.au.

ent active region materials is discussed and compared. The main advantages and disadvantages of these lasers and detectors are also discussed.

II. MIR SEMICONDUCTOR LASERS OPERATING IN THE 2–3 μm REGION

Semiconductor laser has been developed for several decades, first from simple homostructure laser to heterostructure laser, then to double heterostructure (DH) lasers. After that, quantum structures, such as quantum wells (QWs), quantum wires (QWRs), and quantum dots (QDs), have been used as the active region of the laser to enhance the device performance. Quantum cascade laser (QCL) structures have also been adopted as the active region material to make use of intersubband transition to obtain lasers operating in the infrared region of the electric-magnetic spectrum. In this section, we will review the research progress of various lasers techniques operating in the 2–3 μm region.

A. MIR intrinsic interband lasers

The investigation on MIR laser with DH structure started from 1970s. Most of the work was focused on GaSb- and InAs-substrate based Sb-material system, such as AlGaSb, InGaAsSb, AlGaAsSb, and InAsPSb alloy.[2,3] The first RT operated injection DH laser was realized by Caneau *et al.*[4] in 1985, which was grown on GaSb substrate by liquid phase epitaxy (LPE) technique with InGaAsSb/AlGaAsSb DH as the active region. The laser device emitted at the wavelength of 2.2 μm, but worked only in pulsed mode with a threshold current density of 6.9 kA/cm^2.[4] In the meantime, the first injection InAs-based DH MIR laser (InAsPSb alloy as active region) was realized in 1988 with LPE technique by Akiba *et al.*[5] The laser device operated in continuous-wave (CW) mode and emitted at 2.5–2.7 μm, but at low temperature (15–55 K). It should be noted that the lasers fabricated with LPE technique all presented poor device performance, such as low differential quantum efficiency and high threshold current density, which was mainly due to the difficulty in growing thermally metastable materials and multiple layer structures with sharp interface and precise layer thickness. In the following years, more advanced epitaxial growth techniques, such as metalorganic chemical vapor deposition (MOCVD) and molecular beam epitaxy (MBE), were adopted to grow the device structures to improve the device performance. The RT CW operated InGaAsSb/AlGaAsSb/GaSb DH laser was obtained with MBE technology by Choi and Eglash in 1991.[6] The laser emitted at 2.2 μm with an output power of 4.6 mW (at 20 °C). A low threshold current density (J_{th}=940 A/cm^2) was obtained in the pulsed-mode operation.

Though the performance of MIR DH lasers had been improved greatly by utilizing MOCVD and MBE growth techniques, the device performance is still poor compared with the modern QW laser devices. This is mainly due to the poor design of the active region of the laser device. To improve the device performance further, new structures for the active region are highly desirable for the MIR laser devices.

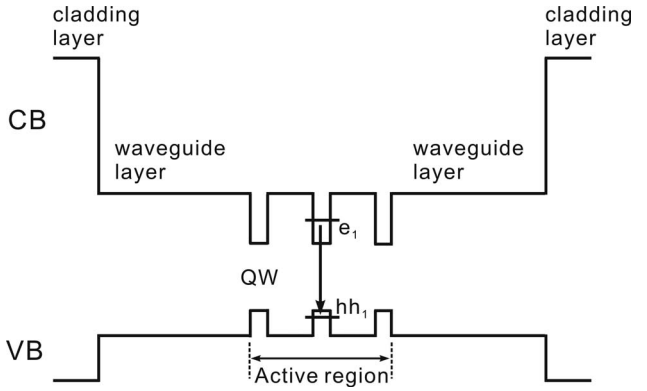

FIG. 1. Band alignment and fundamental electron-hole (e_1-hh_1) transition of type I QW laser. Reproduced from Ref. 13 © 2003 Académie des sciences.

Theoretically, the density of states (DOS) function for electrons in QW system has an abrupt edge that will concentrate electrons in the energy states, which contributes to the laser action, so the efficiency of QW laser will be much higher than that of a bulk material laser, such as DH laser.[7–9] In a QW laser, QW structures (active region) are embedded in waveguide layers, which are usually surrounded by two cladding layers. The waveguide layers have lower band gap energy but higher refractive index compared with the adjacent cladding layers. So, carriers are confined in QW layers while emission beam of the laser is confined inside waveguide layers to prevent it from penetrating into cladding layers, which will enhance the laser performance. Since the first report of RT CW operation of AlGaAs/GaAs QW laser,[10] various groups have done intensive research on QW structures to tune the lasing wavelength and improve the device performance. For MIR QW laser working in the 2–3 μm region, the study is mainly focused on Sb-based QW material system, such as InGaAsSb/AlGaAsSb QWs, etc. In the present section, we will discuss type I QW structure. The band alignment and fundamental electron-hole transition in type I QW structure are shown in Fig. 1. It can be seen that in type I QW structure, both conduction band (CB) edge and valence band (VB) edge of the well layer are located between CB and VB of the barrier layer. So, electrons and holes are confined inside well layers. The first RT CW operated GaSb-based QW laser was obtained by Turner *et al.*[11] in 1994. The InGaAsSb/AlGaAsSb QWs were used for the active region of the laser, leading to an emission wavelength of 2 μm. The laser exhibited a low threshold current density of 143 A/cm^2, high differential quantum efficiency of 47%, and high CW power of 1.3 W. By optimizing the structural parameters of the devices, this kind of type I InGaAsSb/AlGaAsSb QW laser was demonstrated with even better performance, such as high power, high operation temperature (as high as 140 °C), high internal quantum efficiency (~60–80%), and long lifetime (as long as 15 000 h operated in CW mode).[12,13] However, the lasing wavelength of this GaSb-based In(Ga)AsSb/AlGaAsSb QW lasers was all around 2–2.3 μm. Principally, by increasing As or In content in the quaternary alloy In(Ga)AsSb, the lasing wavelength of this GaSb-based type I QW laser can be extended

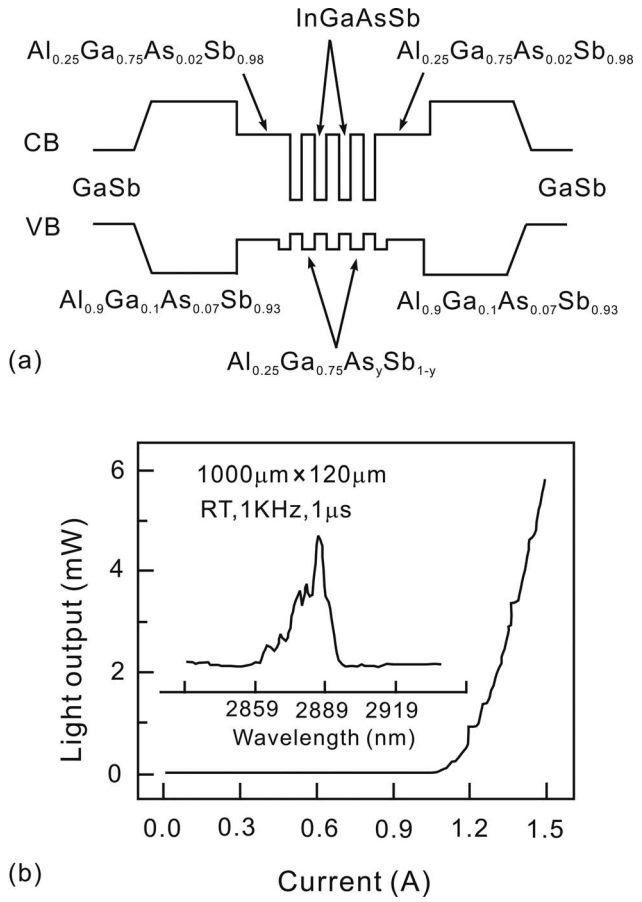

FIG. 2. Band diagram of (a) strain compensated InGaAsSb/AlGaAsSb QW laser and (b) its light-current curves. The inset of (b) shows the RT emission spectrum of the laser. Reproduced from Ref. 17 © 2004 American Institute of Physics.

above 2 μm, even reaching 4.5 μm. However, the performance of this kind of In(Ga)AsSb/AlGaAsSb QW laser degrades somewhat when the emission wavelength is increased to around 2.6 μm. This can be mainly attributed to two factors: one is the inadequate confinement for holes in the Sb-based QW active region, which is induced by the reduction in VB offset of the QWs; the other is the increase in Auger recombination in the active region for the lasers emitting at longer wavelength.[14] When the emission wavelength of this kind of In(Ga)AsSb/AlGaAsSb QW laser is increased, the Auger nonradiative recombination in the QW active region tends to be dominated by the conduction-heavy hole-heavy hole-split off band (CHHS) process (the conduction-to-heavy-hole recombination accompanied by a heavy hole-to-split off band transition), which can be facilitated by the small band gap (E_g) of In(Ga)AsSb alloys.[15] It should be noted that when the emission wavelength is extended beyond 2.6 μm the laser performance deteriorates very fast because of the solid phase miscibility gap of In(Ga)AsSb alloy.[16]

Fortunately, strain-compensated InGaAsSb/AlGaAsSb QWs provide a promising approach to extend the lasing wavelength up to 2.8 μm, and even beyond. In one of the recent works on GaSb-based QW lasers, by using the strain-compensated InGaAsSb/AlGaAsSb QWs as the active region, the lasing wavelength was extended to 2.89 μm at RT.[17] Figure 2(a) schematically illustrates the band configuration of the laser structure where a relatively high arsenic fraction is incorporated in AlGaAsSb barriers so that they are tensile strained. A larger indium fraction can be incorporated in the wells to obtain a narrow band gap since the compressive strain is balanced by the tensile strain in barriers. Meanwhile, the VB of barrier is shifted downward due to the high arsenic fraction so that a better hole confinement is obtained. The laser worked in pulsed mode at RT with a low threshold current density of 920 A/cm^2, and the emission spectrum and light-current curve of laser device is shown in Fig. 2(b). In addition to strain-compensated InGaAsSb/AlGaAsSb QWs, a special growth technique, metamorphic buffer layer, can also be used to extend the emission wavelength of GaInSb/AlGaInSb QWs. By growing GaInSb/AlGaInSb QWs on AlInSb metamorphic buffer layers, the lasing wavelength of GaInSb/AlGaInSb QWs has been successfully extended above 2 μm, even reaching 3.45 μm.[18] However, the performance of this kind of laser has to be improved further.

Beside the In(Ga)AsSb alloy, the III–V–N semiconductor system also provides a promising candidate material for the 2–3 μm MIR devices. The idea of using III–V–N semiconductors for MIR devices comes from developing highly strained InGaAs QWs for MIR devices. InGaAs/InGaAsP/InP and InGaAs/InGaAlAs/InP strained QW lasers operating at 2 and 2.2 μm had been reported by Forouhar *et al.*[19] and Kuang *et al.*,[20] respectively. However, it is difficult to increase the lasing wavelength of InGaAs QWs further. Fortunately, because of the huge bowing parameters induced by the large differences in atomic sizes and electronegativities of N and other group V atoms, incorporating some N element into InGaAs alloy will shift the emission wavelength of InGaAs QWs to a longer wavelength, which is most desirable for the MIR device applications. The band-gap reduction in InGaAs alloy induced by incorporating a few percent of nitrogen was demonstrated by Maier *et al.*[21] and Gokhale *et al.*[22] In principle, the In(Ga)AsN alloys with the energy band gap in the MIR emission region can be lattice matched to GaAs and InP substrates, which shows great advantages over In(Ga)AsSb alloy grown on GaSb substrate. Compared with GaSb substrate, GaAs and InP substrates are more mature and low cost and more suitable for the device fabrication. Moreover, the band-gap reduction and refractive index increase in the III–V–N alloys induced by incorporating small percent of N into the alloy will also enhance the electron/hole confinement and optical confinement, respectively, which is very useful for enhancing the laser performance of QWs.[23] Theoretically, the emission wavelength of In(Ga)AsN alloy grown on GaAs or InP substrates can be extended from 2 to 5 μm by tuning the N concentration in the alloy. The calculated band gap of In(Ga)AsN alloy on GaAs or InP substrates versus nitrogen composition in the In(Ga)AsN alloy is shown in Fig. 3.[23,24] It can be seen that the emission wavelength of In(Ga)AsN alloy can cover the whole MIR region, ranging from 2 to 5 μm, which was also confirmed by the experimental results.[22,25–27] The strained In(Ga)AsN multiple QWs MIR laser was reported recently by Shih *et al.*[28] The laser device emitted at 2.38 μm with a threshold current density of 3.6 kA/cm^2 in pulsed mode at

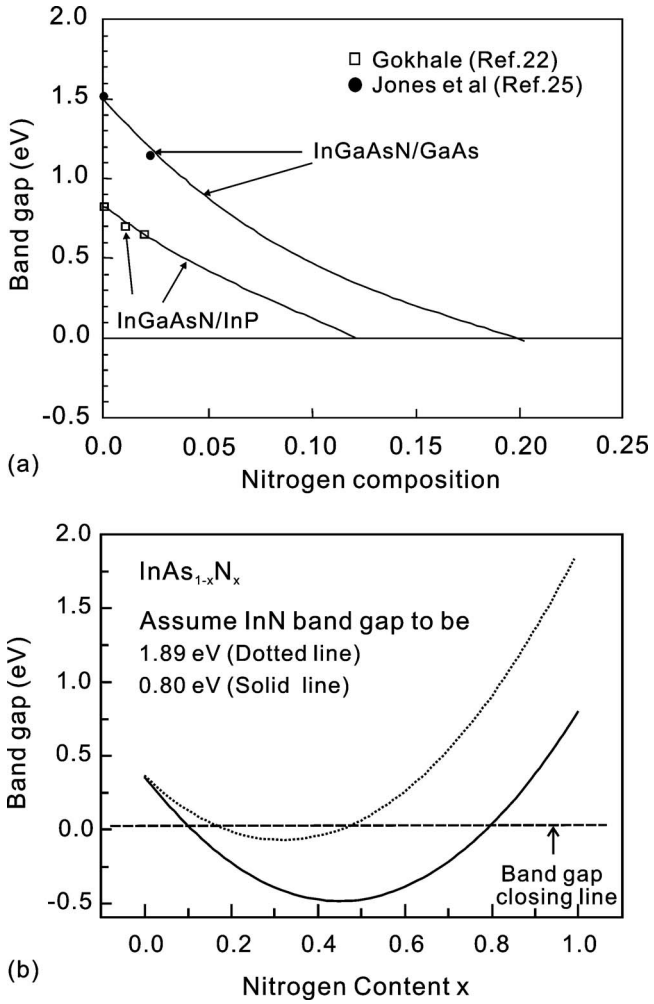

FIG. 3. Calculated band gap of (a) InGaAsN and (b) InAsN alloy vs N composition. In (a), the theoretical calculations (bold lines) are done at $T=0$ K and compared with low-temperature experiments for both GaAs- and InP-based systems (Refs. 22 and 25). In (b), the dotted line and solid line are calculated by assuming InN band gap as 1.89 and 0.80 eV, respectively. Reproduced from Ref. 23 © 2007 Elsevier Ltd., and Ref. 24 © 1999 American Institute of Physics.

260 K, where the light-current curves and emission spectrum of the laser are shown in Fig. 4. This demonstrated that the III–V–N alloys provide a promising way to develop high performance MIR lasers. To achieve theoretically predicted MIR lasers based on this system, many material science issues need to be addressed in this III–V–N alloy system.

B. MIR type II QW lasers

As discussed in Sec. II A, a main factor limiting the performance of type I QW laser with small band-gap energy is the Auger nonradiative recombination in the device structure. To reduce Auger nonradiative recombination rate in the QW lasers, type II QW structure was proposed for the active region of the laser devices. Figure 5 shows the schematic band alignment of typical type II QW structure.[29] The CB edge of QW layer is placed between CB and VB of the barrier. The electrons and holes confined in QW structures are separated spatially, and the radiative recombination corresponds to the transitions between CB electrons in QW layer and VB holes in barrier layer. Although the efficiency

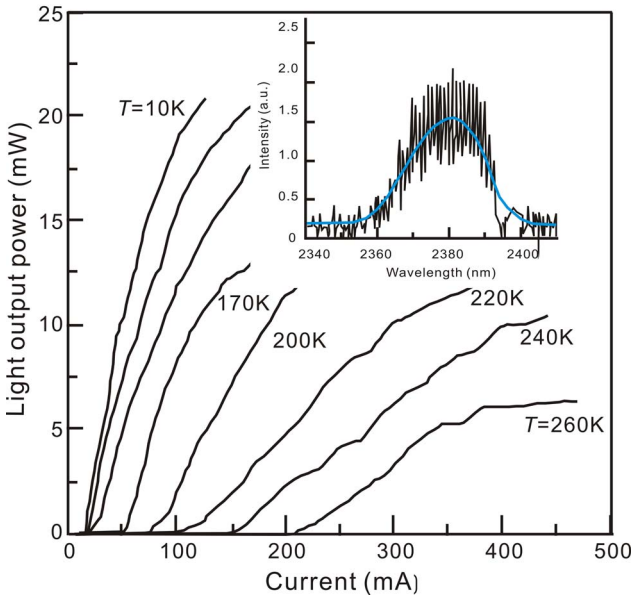

FIG. 4. (Color online) Light-current curves of strained InAsN/InGaAs QW laser. The inset shows the emission spectrum of the laser under injection current $I=1.4\ I_{th}$ at 260 K. Reproduced from Ref. 28 © IEE, 2003.

of radiative recombination in type II QWs is reduced due to the decreased wave function overlap between the spatially separated electrons and holes, it has been demonstrated that, under injection, the localized electrons in QW can pull the holes from the adjacent barriers due to Coulomb interaction. The holes in barriers are mainly confined in the nearly triangular potential wells adjacent to QW interfaces. So, the probability for the holes to be present near QW is increased, which increases the overlap of electron-hole wave functions.

At present, the study of type II MIR QW laser is mainly focused on InAs-GaSb-AlSb material family. The first type II QW laser working in the 2–3 μm range at RT was reported in 1996 by Baranov *et al.*[30] The laser device was grown on GaSb substrate and used the InGaAsSb/GaSb multiquantum wells (MQWs) as the active region. The laser emitted at 2.36 μm with a threshold current density of 305 A/cm^2 in pulsed mode. Soon after that, the RT CW operating type II InGaAsSb/GaSb QW laser was demonstrated, which emitted

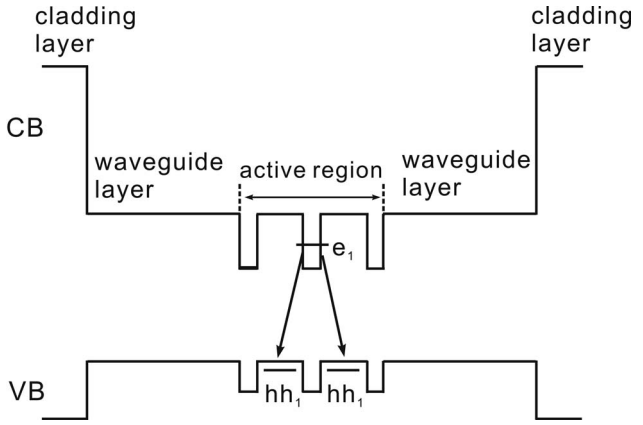

FIG. 5. Band alignment and fundamental electron-hole (e_1-hh_1) transition of type II QW laser. Reproduced from Ref. 13 © 2003 Académie des sciences.

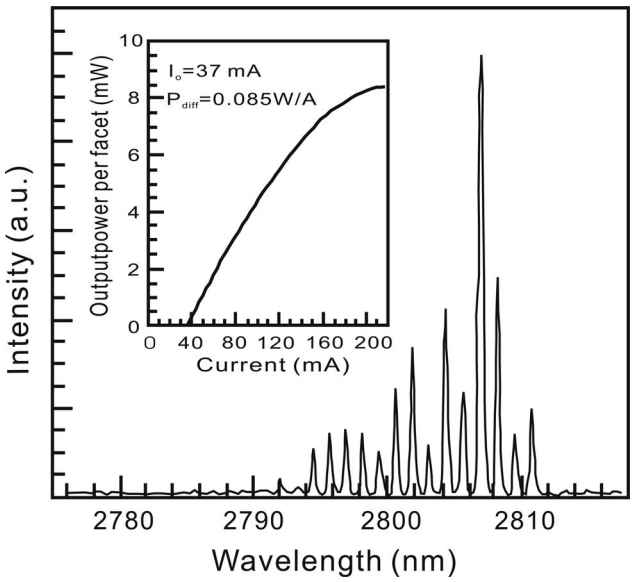

FIG. 6. CW operation spectrum of type II InGaAsSb/ GaSb QW laser under an injection current of $I=1.5\ I_{th}$. The inset shows current-output power characteristic of the laser with a threshold current of 37 mA. Reproduced from Ref. 32 © 2006 IEEE.

at 2.38 μm with a low threshold current (60–150 mA).[31] By optimizing the material parameters and device structure, the performance of the InGaAsSb/GaSb QWs based MIR laser was further enhanced. Under the condition of RT CW operation, the threshold current of the InGaAsSb/GaSb QW laser, which emitted at 2.8 μm, was reduced to 37 mA, and the output power was increased to 8 mW per facet of an uncoated 800×7 μm^2 ridge waveguide laser, where the emission spectrum and current-output power curves are shown in Fig. 6.[32] Recently, hole-well type II QW laser structure was proposed to increase the confinement of holes to enhance the quantum efficiency of the laser.[33] In this kind of laser structure, only holes are confined in the QWs. The injection hole-well type II laser was also demonstrated most recently by Cerutti *et al.*[34] The schematic band diagram and the emission spectra of the hole-well laser are shown in Fig. 7. The laser device used the GaSb-based type II InGaSb/InGaAsSb MQWs as the active region and emitted at 2.93 μm in pulsed mode at 243 K, indicating that hole-well QWs also provide a promising way to fabricate MIR laser.

To achieve the lasers emitting in the 2–3 μm region, a wide variety of materials with type I and type II QW structures have been investigated. All the traditional type I and II QW lasers have presented excellent performance at low temperature. However, their RT performances are far from satisfactory. To achieve high operation temperature, a special type II QW structure was also proposed for MIR laser device, which is usually called interband type II broken gap InAs/InGaSb/InAs "W" laser (or type III QW laser). The designed active region is made up of several QW periods, and each period includes a "hole" QW sandwiched by a double "electron" QWs, leading to the formation of W shape. The schematic band diagram of this kind of laser structure is shown in Fig. 8.[35] Besides keeping the characteristics of type II QWs (e.g., reduction in the Auger recombination and internal losses), type III lasers can increase the electron-hole

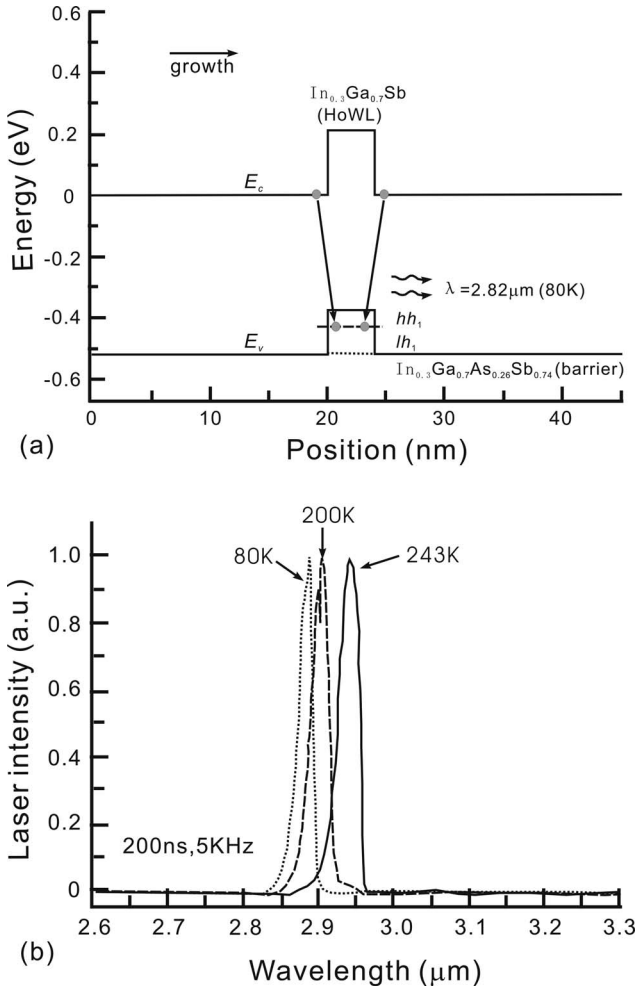

FIG. 7. Schematic band diagram of (a) the InGaSb/InGaAsSb hole-well laser and (b) the emission spectra of the laser at 80, 200, and 243 K. Reproduced from Ref. 34 © The Institute of Engineering and Technology 2006.

overlap integral and hence the optical matrix elements, giving values comparable to that of type I QW structures. With this W QW structure, the lowest energy of indirect radiative transitions in the W type QW can be, in principle, reduced to zero by increasing the QW width. The RT quasi-CW operating W QW MIR laser was first obtained by Baranov *et al.*[36] The laser used the InAs/GaSb QWs as the active region and emitted at 2.32 μm with a threshold current density of 7.9 kA/cm^2.

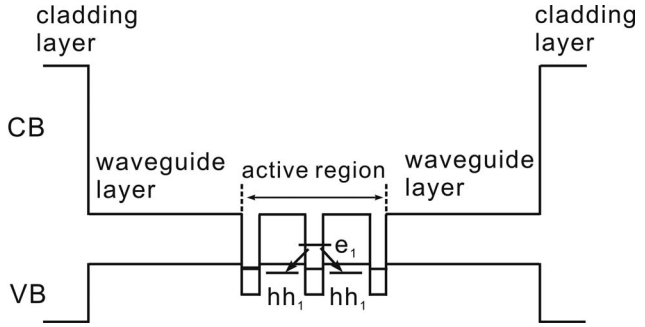

FIG. 8. Band alignment and fundamental electron-hole (e_1-hh_1) transition of type III QW laser. Reproduced from Ref. 13 © 2003 Académie des sciences.

Besides GaSb- or InAs-based type II QWs, InP-based type II superlattices (SLs) were also proposed for the MIR laser application recently.[37] Surely, this InP-based laser structure will be much easy to fabricate, compared with GaSb- or InAs-based materials. The laser used the InGaAs/GaAsSb SLs as the active region and worked at 1.71 μm in CW mode at RT.

In all, to improve the performance of type II QW MIR lasers, it is very important to increase the overlap of carrier wave function with minimized internal absorption loss and reduced Auger recombination in the design of type II QW active region.

C. MIR QC lasers

Since the demonstration of the first electrically pumped quantum cascade (QC) intersubband laser at 4.2 μm in 1994, the QCL has been intensively investigated for mid- and far-infrared laser application.[38] The QCL is based on cascaded unipolar intersubband or interband transitions. Also, the QC structures rely on recycling of the electrons to increase the optical gain, which allow very high quantum efficiency (higher than 100%) lasers.[39] Based on the carrier transitions in the QC structure (intersubband and interband), the MIR QCLs can be divided into two groups: intersubband and interband QC lasers.

1. MIR intersubband QC lasers

The intersubband QC structure has been proved to be suitable for fabricating mid- and far-infrared laser devices. The lasing wavelength above 4 μm can be obtained comparatively easily by choosing appropriate well material with appropriate well width as the active region of the laser device.[40] However, it is quite difficult to obtain a short lasing wavelength with intersubband QC structures (e.g., 2–3 μm). The point is that in intersubband QCLs, the optical gain is realized by electron-electron transitions in CB. By resonant tunneling through a potential barrier, electrons are injected into the upper state of the laser transition region, and electrons in the lower energy state tunnel out from the well region to realize the population inversion. Then, the CB discontinuity (ΔE_c) between the barrier and well layer should be much larger than the intersubband transition energy to prevent electron leakage from the QW. So, the CB band offset (ΔE_c) limits how short the lasing wavelength we can achieve. At present, the study on MIR intersubband QC laser is mainly focused on the In(Ga)As/In(Al)As material system. By growing strain-balanced InGaAs/InAlAs QC structures on InP substrate, QCL emitting at 3.4 μm was demonstrated in 1998.[41] However, no progress was made in the following several years. The long-term absence of advances in the direction to shorter wavelength despite remarkable progress in QCLs toward slightly longer wavelength indicates that this result (3.4 μm lasing wavelength) is close to the short wavelength limit for this material system. So, new material system should be considered to develop the QCL working in the 2–3 μm region. The InAs/AlSb material system, which can be grown on InAs or GaSb substrates, seems to be the most promising candidate materials to further reduce the QCL emission wavelength.[42] This material system provides a large ΔE_c of 2.1 eV, small electron effective mass of the well material ($m^*=0.023m_0$ for InAs), and large separation between direct and indirect minima of the CB of the well material (0.72 to 0.76 eV), which is of particular interest for developing short-wavelength QCLs. By growing InAs/AlSb SLs on *n*-type InAs substrate, the QC laser emitting below 3 μm was obtained.[42] The lasers emitted at 2.95–2.97 μm in pulsed mode with threshold current densities near 3 kA/cm^2 at 84 K and could operate up to RT. Further optimization of the device design and growth parameters is very desirable to improve the performance of such kind of InAs/AlSb QC laser.

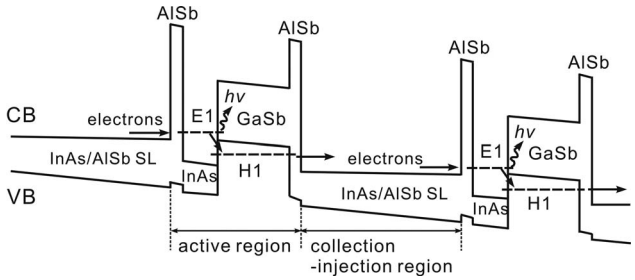

FIG. 9. Band diagram (not to scale) under bias of a QCL based on interband transitions in an AlSb/InAs/GaSb QW structure. Reproduced from Ref. 13 © 2003 Académie des sciences.

In the meantime, GaN-based QWs or SLs can also provide large ΔE_c, which also can be used for the fabrication of MIR QC laser working in the 2–3 μm region. By growing GaN/AlGaN SLs, intersubband absorption wavelength of 1.52–4.2 μm had been obtained.[43] Intraband absorption in the range of 2–4 μm had also been observed in the AlInN/GaN MQWs.[44] Besides these, intersubband absorption in the range of 1.5–3.5 μm had also been achieved for the GaN/AlN MQWs.[45] However, though intersubband absorption in the 2–3 μm range has been observed for these GaN-based QWs, no GaN-based QC lasers operating in the 2–3 μm range have been demonstrated, which presents a subject for future study.

2. MIR interband QC lasers

As for the intersubband QC laser, one detrimental factor limiting the performance of intersubband MIR QC lasers is the fast carriers' nonradiative relaxation between the subbands via optical phonon scattering. This leads to low radiative efficiency and substantial heating of the devices. Fortunately, interband QC laser provides a good opportunity to suppress the nonradiative relaxation between the subbands, and thus increases the radiative efficiency greatly. In interband QC laser structures, the optical gain is realized through the resonant interband tunneling in a type III broken-gap system, which has been discussed in Sec. II B. Figure 9 shows the schematic band diagram of the AlSb/InAs/GaSb interband QC laser.[13,46] First, the electrons tunnel from the injection region (InAs/AlSb SLs) into InAs QWs. Then, they are blocked by the GaSb and AlSb barriers that prevent them from tunneling to the next collection/injection region and may escape only by making optical transitions to the VB of the GaSb QW. Finally, they transfer to the collection region

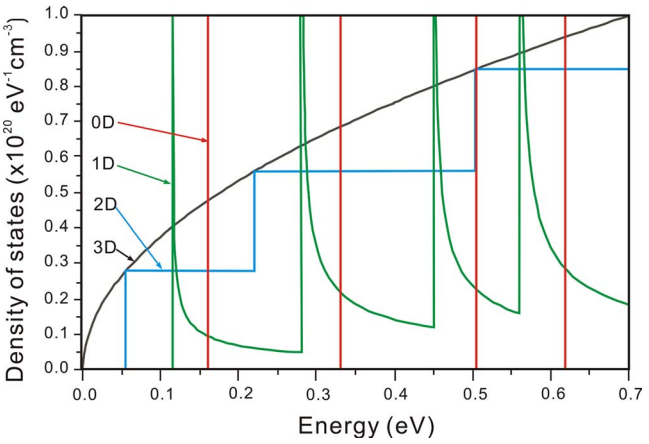

FIG. 10. (Color online) Density of electron states for bulk material (3D), QW (2D), QWR (1D), and QD (0D).

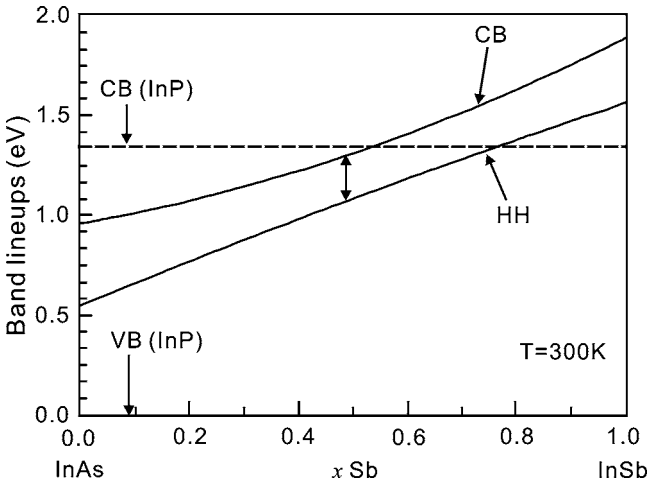

FIG. 11. Variation in the band lineups at $T=300$ K as a function of Sb concentration in a bulk strained $InAs_{1-x}Sb_x$ alloy grown on InP substrate, relative to the InP VB. The variation in $InAs_{1-x}Sb_x$ CB and heavy hole band edge energies are represented by straight lines. Reproduced from Ref. 52 © 2005 American Institute of Physics.

through elastic interband tunneling. By optimizing the device parameters, interband QC lasers with good performance had been obtained, which emitted at 3.3–3.5 μm. The laser worked up to 300 K in pulsed mode and 150 K in CW mode and exhibited a threshold current density as low as 13.2 A/cm^2 and power efficiency as large as 17% under CW conditions at 80 K.[47] However, it also presents a big challenge to shift the lasing wavelength of the interband QC laser below 3 μm, which requires new material system.

D. MIR QD lasers

Recently, QD laser appears to be the most promising high performance semiconductor laser for the next generation optical systems. Figure 10 shows the DOS distribution versus dimensionality. It is obvious that the DOS of QD is much narrower compared with that of bulk material and QW, which forms the basis for improved device performance. Theoretically, QD laser will have a reduced threshold current, increased differential efficiency, high speed operation, and high operation temperature. Different QD material systems have been developed to fabricate QD lasers. To date, most of the work is focused on QD laser operating at 1.3 and 1.55 μm. Also, high performance QD lasers emitting at 1.3 and 1.55 μm have been realized.[48,49] Although some special growth techniques have been adopted to increase the emission wavelength of GaAs- and InP-based InAs QDs and quantum dashes close to 2 μm,[50] it still presents a big challenge to extend the lasing wavelength above 2 μm for In(Ga)As QDs on GaAs and InP substrates. As discussed in Sec. II A, dilute nitride QDs, such as In(Ga)AsN QDs on InP or GaAs substrates, will provide a potential candidate material for the QD laser operating in the 2–3 μm range due to their low band gap energy. Besides the dilute nitride QDs, the In(As)Sb QDs on InAs and GaSb substrates also show a possible way to shift the lasing wavelength into the 2–3 μm range. InSb/GaSb QDs with 3.5 μm photoluminescence (PL) wavelength had been reported.[51] Because of the mature processing technology of InP-based materials, InAsSb QDs on InP substrate appear as the most promising and competing material for the QD laser working in the 2–3 μm range. Figure 11 shows the variation in band lineups at 300 K as a function of Sb concentration in a bulk strained InAsSb alloy grown on an InP substrate (the energy values are given relative to the InP VB energy).[52] Obviously, the emission wavelength of strained InAsSb alloy on InP can be extended to 2–3 μm, even to 5 μm. Some work has been done on InP-based InAsSb QDs. Although InAsSb/InGaAs/InP QDs with 2.35 μm PL wavelength had been reported,[53] the lasing wavelength was still around 2 μm.[54] It is a big challenge to extend the emission wavelength of InAsSb QD laser above 2 μm. Further work is highly desirable to improve the material quality to achieve high performance InAsSb QD lasers operating in the 2–3 μm region.

III. MIR PHOTODETECTORS OPERATING IN THE 2–3 μm REGION

Among the materials studied for the detection in the MIR region, three main kinds of photodetectors are available currently: interband absorption detectors, QW infrared photodetectors (QWIPs), and QD infrared photodetectors (QDIPs). The latter two groups are based on the intersubband transition of carriers in the device structures.

A. MIR interband absorption photodetectors

1. InSb photodiodes

InSb photodiodes have been developed for more than 50 years. Usually, the InSb photodiodes are fabricated from bulk InSb wafers, and the *p-n* junction is formed by impurity diffusion and ion implantation.[55] Fabricated InSb photodiodes have a typical R_0A product of $\sim 10^6$ Ω cm^2 and peak detectivity of 10^{11}–10^{12} cm $Hz^{1/2}/W$ at 77 K.[56] Because InSb is a more mature material than other IR detector materials, it has received the most attention for the focal plane array (FPA) applications. High performance InSb photodetectors are commercially available now.

As for the InSb photodetector research, there is a new trend—that is to grow InSb films on GaAs or GaAs-coated Si substrates.[56,57] Such structures will take advantages of

both high quantum efficiency of narrow-gap semiconductors and advanced integrated circuit technologies, thus providing opportunities to develop monolithic integrated devices.

2. InAsSb photodiodes

InAsSb material has a strong potential for developing MIR detectors operating in the wavelength range of 2–5 μm, as discussed in Sec. II D. The best performance of conventional InAsSb photodiodes can be obtained with lattice-matched $InAs_{1-x}Sb_x/GaSb$ $(0.10 \leq x \leq 0.14)$ structure.[58] The backside-illuminated $InAs_{0.86}Sb_{0.14}/GaSb$ photodiodes fabricated with LPE technique can cover the spectral range of 1.7–4.2 μm. However, most of the work in this field is focused on developing detector with the detection wavelength above 3 μm. Less attention has been devoted to the detectors operating in the 2–3 μm range.

3. InGaAs photodiodes

Besides Sb-based materials, the ternary InGaAs material can also cover the wavelength range of 2–3 μm. Principally, the band gap of $In_xGa_{1-x}As$ ternary system spans from 0.35 eV (3.5 μm) for InAs to 1.43 eV (0.87 μm) for GaAs.[59] So, the InGaAs material is suitable for fabricating photodetector working in the range of 1–3 μm. Meanwhile, for InGaAs materials, a more mature growth and processing technology can be relied on and better performance of the photodetector could be expected. The photodetectors using $In_{0.53}Ga_{0.47}As$ material lattice matched to InP substrate with a detection wavelength of 1.55 μm have been widely used in optical communication systems and other fields for decades. To shift the detection wavelength into the 2–3 μm range, more In content should be incorporated into the InGaAs alloy. However, this presents a challenge. The high In concentration in InGaAs alloy will induce a large lattice mismatch between InGaAs layer and InP substrate. So, some buffer layer should be inserted to prevent the large mismatch between InGaAs layer and InP substrate. By using a linear graded $In_xGa_{1-x}As$ buffer layer (x value ranges from 0.53 to 0.8), the $In_{0.8}Ga_{0.2}As$ active layer was grown on InP substrate by Gas Source MBE, which allowed to extend the cutoff wavelength of InGaAs photodetector to 2.5 μm at RT.[60]

B. MIR QW photodetectors

1. MIR type I QW detectors

The QWIPs are based on the intersubband absorption in QWs. QWIPs have a narrow absorption spectrum that can be tuned to match any transition in various wavelength range by adjusting the QW width, QW layer composition, and barrier layer composition. Moreover, it can be fabricated with mature III–V semiconductor processing technology based on GaAs and InP substrates. By stacking several different QW structures together, multicolor detector can also be obtained.[61,62]

Because QWIP is based on the intersubband transition in QWs, it is easy to fabricate QWIPs working in the long-wavelength range. To obtain QWIP working in short wavelength regions, QWs with large ΔE_c should be considered. By using AlAs/GaAs MQWs, the detection wavelength could be pushed to around 3 μm.[63] In order to get even short response wavelength, new QW materials with even larger ΔE_c are highly desirable. Dilute-N alloys show some promise to achieve this goal. By using dilute-N alloy as the QW layer and larger band-gap material as barrier layer, the detection wavelength of QW photodetector could be pushed to 3 μm, even shorter. As discussed in Sec. II C 1, GaN-based QWs exhibit a large ΔE_c, which can also be used to shift the detection wavelength into the 2–3 μm region. However, no GaN-based QW detectors working in the 2–3 μm region have been demonstrated until now. Further work should be done on this material system to achieve intersubband detectors operating in the 2–3 μm region, which presents a subject for future study.

2. MIR type II superlattice detectors

As discussed in Sec. III B 1, it is difficult to tune the detection wavelength of intersubband QW detector into the 2–3 μm range. However, as shown in Sec. II B, the interband transition in type II QWs may provide a promising way to fabricate the photodetectors working in the 2–3 μm region. Like type II QW lasers, the type II QW detector can also reduce the Auger recombination rate of carriers in the device structure, which will enhance the operation temperature of QW detectors. Similarly, in type II QW detector, although electrons and holes are mostly confined in different layers, their wave functions can extend through the barriers. So, the overlap of the electron and holes wave functions is not zero. Therefore, the optical matrix element in the region near the interfaces is big enough for a considerable optical absorption. Although type II QWs will exhibit a low absorption efficiency than type I QWs, the spatial separation will reduce the Auger recombination rate, and the generated electron-hole pair will survive longer, which will enhance the operation temperature of type II QW detector.[57]

By using this kind of type II QWs as the active layer (e.g., InAs/Ga(In)Sb SLs), the detection wavelength of the detector can be pushed to 2 μm. For the InAs/Ga(In)Sb SLs detector, it is possible to tune the SLs band gap into the 2–3 μm range by controlling the thickness of InAs layer,[64,65] which provides a subject for future study.

C. MIR QD photodetectors

Like QW photodetector, QD photodetector also utilizes the intersubband transition to generate photoresponse. Meanwhile, because of the special DOS distribution, QDs have intrinsically several advantages over QWs for infrared detector applications. QDIPs will have much higher efficiency because of the lower LO phonon scattering rate in QDs compared to the QWs. Moreover, the dispersionless energy levels in QDs reduce the thermal generation rate of the free carriers, which can enhance the operation temperature. In addition, QDs are sensitive to the normal incident light due to the breaking of polarization selection rules.

Since the first report of (In,Ga)As/GaAs QDIPs,[66] the device performances have been enhanced greatly. RT operating QDIPs have been realized recently by Lim *et al.*[67] The devices were grown on InP substrates with dot in well struc-

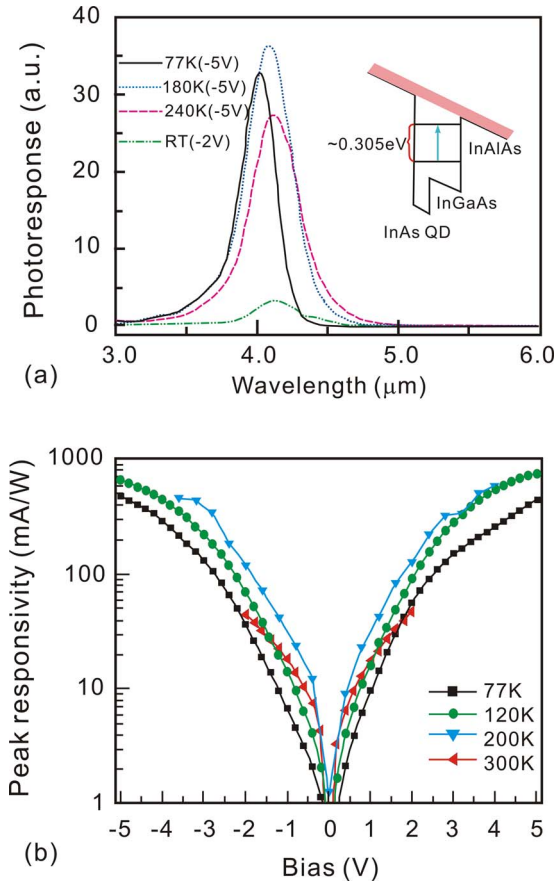

FIG. 12. (Color online) (a) Photoresponses at different temperatures (−5 V bias for 77, 180, and 240 K and −2 V bias for RT) and (b) peak responsivity at different temperatures as a function of applied bias of InAs/InGaAs QD in QW MIR photodetector. The inset of (a) shows the related intraband transition involved. Reproduced from Ref. 67 © 2007 American Institute of Physics.

ture (InAs QDs in InGaAs QW) as the active layer. The peak detection wavelength was around 4.1 μm and the RT detectivity about 6.7×10^7 cm $Hz^{1/2}/W$, where the photoresponses and peak responsivity of the detector are shown in Fig. 12. By using this kind of InAs/InGaAs QDIPs, a 320 $\times$256 infrared FPA operated at temperatures up to 200 K was demonstrated.[68] The FPA had a peak detection wavelength of 4 μm, a responsivity of 34 mA/W, a conversion efficiency of 1.1%, and a noise equivalent temperature difference of 344 mK at an operating temperature of 120 K. Figure 13 shows the images taken at 130 and 200 K with the QDIP FPA. Also, by adopting different intersubband transitions (bound to bound and bound to continuum transitions) in the QDIPs, multicolor detection in one detector can be achieved. By using dot in well (InAs dots in InGaAs well) structure as the active layer, three-color InAs/InGaAs QDIPs with center wavelengths at 3.8, 8.5, and 23.2 μm were realized by Krishna *et al.*[69] The shorter wavelength responses (3.8 and 8.5 μm) were attributed to bound-to-continuum and bound-to-bound transitions between the states in the dots and the states in the well, whereas the longer wavelength response (23.2 μm) was ascribed to intersubband transition between the energy levels in the QDs, where the photoresponses are shown in Fig. 14.

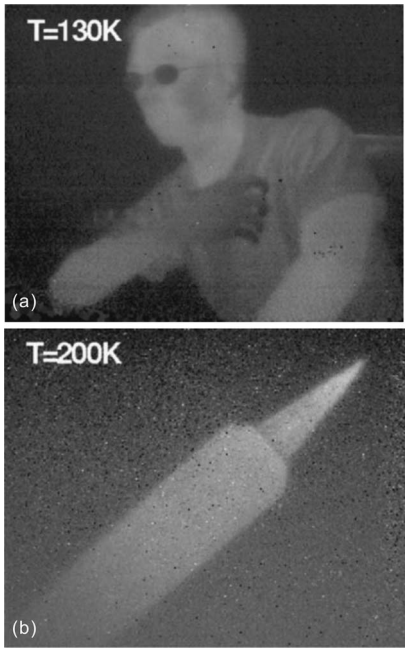

FIG. 13. Focal plane array imaging taken with InAs/InGaAs/InP QD in QW MIR photodetectors at 130 and 200 K. Reproduced from Ref. 68 © 2007 American Institute of Physics.

However, most of the work in this field is focused on the QDIPs operating above 3 μm. Like QW photodetector, the detection wavelength of QDIP is also limited by the CB offset ΔE_c (similarly, VB offset ΔE_v for the *p*-type QDIP). By tuning ΔE_c in the QDIP structure, the detection wavelength of the detector can be shifted into the 2–3 μm range, which can be realized by choosing QDs with appropriate material system as the active layer of the detector. For example, InAs, Sb-based, and dilute N-based semiconductor QDs grown on matrix with large band gap (e.g., GaAs, AlGaAs, etc.), and GaN-based QDs can provide potential candidate materials for the QDIPs operating in the 2–3 μm range, which presents an exciting subject for future study.

IV. SUMMARY

Several materials and structures can be used to obtain the MIR (2–3 μm) lasers and photodetectors. For the laser application in shorter MIR wavelength range (2–2.6 μm),

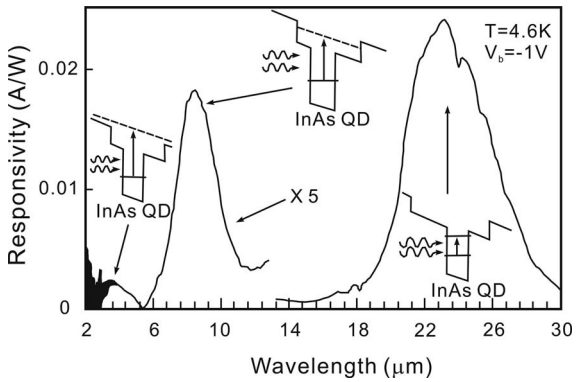

FIG. 14. Photoresponse of the three-color InAs/InGaAs QD in QW photodetector. The insets show the related intraband transitions involved. Reproduced from Ref. 69 © 2003 American Institute of Physics.

Sb-related type I QW lasers appear to be the promising system. Because in this wavelength range, the Auger nonradiative recombination in the active region can be well suppressed due to the disappearance of the resonance between the effective band-gap CH and the spin split-off energy transition HS. For longer MIR wavelength laser application (2.6–3 μm), the Sb-based type II QW lasers provide an attractive choice, which can suppress the Auger recombination in the QW device structure. However, the device structure and material parameters of both type I and type II QW lasers should be optimized to improve their performance further. As for QC lasers, the traditional material systems, such as In(Ga)As/In(Al)As intersubband QC laser and InAs/AlSb interband QC laser, seem to be unsuitable for the 2–3 μm laser applications. So, it is very important to find new material systems (e.g., InAs/AlSb SLs, GaN-based materials) as the active region of the QC lasers. The most promising candidates for MIR laser operating in the 2–3 μm range are the QW and QD laser based on III–V–N and InAsSb materials, which can be grown on the mature InP or GaAs substrates.

For MIR photodetectors operating in the 2–3 μm region, the performance of the traditional InAsSb and InGaAs photodiodes should be improved further, which can be achieved by optimizing the device structure and tuning the material composition. For type I QWIPs working in the 2–3 μm region, the key is to find the material with large ΔE_c as the active region. In this respect, the GaN-based QWs may exhibit great potential. In addition, InAs/GaSb type II QWIPs may also be used for the 2–3 μm infrared detection. The most important technique for the 2–3 μm infrared detection applications is the QDIPs based on the InAs, Sb- and N-related materials.

ACKNOWLEDGMENTS

Thanks are due to Australian Research Council for the financial support. We thank all our collaborators and coworkers for fruitful discussions. Special thanks are due to our collaborators, Dr. Ken Grant, Dr. Bradley Clare, and Dr. Kerry Mudge, and our ANU colleagues, Dr. H. H. Tan, Dr. L. Fu, Dr. Q. Gao, and Dr. Q. Li.

[1] I. S. Glass, *Handbook of Infrared Astronomy* (Cambridge University Press, Cambridge, 1999), pp. 28–33.
[2] M. S. Bresler, O. B. Gusev, N. V. Zotova, M. Aydaraliev, S. A. Karandashev, B. A. Matveev, N. M. Stus', and G. N. Talalakin, Opt. Mater. (Amsterdam, Neth.) **6**, 111 (1996).
[3] P. Grunberg, A. Baranov, C. Fouillant, J. L. Lazzari, P. Grech, G. Boissier, C. Alibert, and A. Joullié, Electron. Lett. **30**, 312 (1994).
[4] C. Caneau, A. K. Srivastava, A. G. Dentai, J. L. Zyskind, and M. A. Pollack, Electron. Lett. **21**, 815 (1985).
[5] S. Akiba, Y. Matsushima, T. Iketani, and M. Usami, Electron. Lett. **24**, 1069 (1988).
[6] H. K. Choi and S. J. Eglash, Appl. Phys. Lett. **59**, 1165 (1991).
[7] Zh. I. Alferov, ChemPhysChem **2**, 500 (2001).
[8] B. Zhao, T. R. Chen, and A. Yariv, Electron. Lett. **27**, 2343 (1991).
[9] Y. Arakawa, K. Vahala, and A. Yariv, Appl. Phys. Lett. **45**, 950 (1984).
[10] R. D. Dupuis, P. D. Dapkus, R. Chin, N. Holonyak, Jr., and S. W. Kirchoefer, Appl. Phys. Lett. **34**, 265 (1979).
[11] G. W. Turner, H. K. Choi, D. R. Calawa, J. V. Pantano, and J. W. Chludzinski, J. Vac. Sci. Technol. B **12**, 1266 (1994).
[12] D. Donetsky, G. Kipshidze, L. Shterengas, T. Hosoda, and G. Belenky, Electron. Lett. **43**, 810 (2007); G. Belenky, D. Donetski, L. Shterengas, T. Hosoda, J. F. Chen, G. Kipshidze, M. Kisin, and D. Westerfeld, Proc. SPIE **6900**, 690004 (2008).
[13] D. A. Yarekha, G. Glastre, A. Perona, Y. Rouillard, F. Genty, E. M. Skouri, G. Boissier, P. Grech, A. Joullié, C. Alibert, and A. N. Baranov, Electron. Lett. **36**, 537 (2000); A. Joullié and P. Christol, C. R. Phys. **4**, 621 (2003).
[14] H. K. Choi, G. W. Turner, M. J. Manfra, and M. K. Connors, Appl. Phys. Lett. **68**, 2936 (1996); H. K. Choi, G. W. Turner, and H. Q. Le, *ibid.* **66**, 3543 (1995).
[15] J. R. Meyer, C. A. Hoffman, F. J. Bartoli, and L. R. Ram-Mohan, Appl. Phys. Lett. **67**, 757 (1995).
[16] J. L. Lazzari, E. Tournié, F. Pitard, A. Joullié, and B. Lambert, Mater. Sci. Eng., B **9**, 125 (1991).
[17] W. Li, J. B. Héroux, H. Shao, and W. I. Wang, Appl. Phys. Lett. **84**, 2016 (2004).
[18] E. A. Pease, L. R. Dawson, L. G. Vaughn, P. Rotella, and L. F. Lester, J. Appl. Phys. **93**, 3177 (2003).
[19] S. Forouhar, A. Ksendzov, A. Larsson, and H. Temkin, Electron. Lett. **28**, 1431 (1992).
[20] G. K. Kuang, G. Böhm, N. Graf, M. Grau, G. Rösel, R. Meyer, and M.-C. Amann, Electron. Lett. **36**, 1849 (2000).
[21] M. Maier, D. Serries, T. Geppert, K. Köhler, H. Güllich, and N. Herres, Appl. Surf. Sci. **203–204**, 486 (2003).
[22] M. R. Gokhale, J. Wei, H. Wang, and S. R. Forrest, Appl. Phys. Lett. **74**, 1287 (1999).
[23] Z. Y. Yin and X. H. Tang, Solid-State Electron. **51**, 6 (2007).
[24] L. Bellaiche, Appl. Phys. Lett. **75**, 2578 (1999).
[25] E. D. Jones, N. A. Modine, A. A. Allerman, S. R. Kurtz, A. F. Wright, S. T. Tozer, and X. Wei, Phys. Rev. B **60**, 4430 (1999); E. D. Jones, N. A. Modine, A. A. Allerman, I. J. Fritz, S. R. Kurtz, A. F. Wright, S. T. Tozer, and X. Wei, Proc. SPIE **3621**, 52 (1999).
[26] I. Vurgaftman, J. R. Meyer, and L. R. Ram-Mohan, J. Appl. Phys. **89**, 5815 (2001).
[27] J. Wu, W. Walukiewicz, K. M. Yu, J. W. Ager III, E. E. Haller, H. Lu, W. J. Schaff, Y. Saito, and Y. Nanishi, Appl. Phys. Lett. **80**, 3967 (2002).
[28] D. K. Shih, H. H. Lin, and Y. H. Lin, IEE Proc.: Optoelectron. **150**, 253 (2003).
[29] P. Christol, P. Bigenwald, A. Joullié, Y. Cuminal, A. N. Baranov, N. Bertru, and Y. Rouillard, IEE Proc.: Optoelectron. **146**, 3 (1999).
[30] A. N. Baranov, Y. Cuminal, G. Boissier, C. Alibert, and A. Joullié, Electron. Lett. **32**, 2279 (1996).
[31] A. Joullié, Y. Cuminal, A. N. Baranov, D. Bec, J. C. Nicolas, P. Grech, Y. Rouillard, G. Glastre, and R. Blondeau, Proceedings of the 16th IEEE International Semiconductor Laser Conference, NARA, Japan, 5–10 October 1998 (unpublished).
[32] K. Rößner, M. Hümmer, T. Lehnhardt, M. Müller, A. Forchel, M. Fischer, and J. Koeth, IEEE Photonics Technol. Lett. **18**, 1424 (2006).
[33] A. P. Ongstad, R. Kaspi, M. L. Tilton, J. R. Chavez, and G. C. Dente, J. Appl. Phys. **98**, 043108 (2005).
[34] L. Cerutti, G. Boissier, P. Grech, A. Pérona, J. Angellier, Y. Rouillard, R. Kaspi, and F. Genty, Electron. Lett. **42**, 1400 (2006).
[35] M. E. Flatté, J. T. Olesberg, S. A. Anson, T. F. Boggess, T. C. Hasenberg, R. H. Miles, and C. H. Grein, Appl. Phys. Lett. **70**, 3212 (1997).
[36] A. N. Baranov, N. Bertru, Y. Cuminal, G. Boissier, C. Alibert, and A. Joullié, Appl. Phys. Lett. **71**, 735 (1997).
[37] M. Peter, R. Kiefer, F. Fuchs, N. Herres, K. Winkler, K. H. Bachem, and J. Wagner, Appl. Phys. Lett. **74**, 1951 (1999).
[38] J. Faist, F. Capasso, D. L. Sivco, C. Sirtori, A. L. Hutchinson, and A. Y. Cho, Science **264**, 553 (1994).
[39] R. Q. Yang, J. D. Bruno, J. L. Bradshaw, J. T. Pham, and D. W. Wortman, Electron. Lett. **35**, 1254 (1999).
[40] K. Ohtani, Y. Moriyasu, H. Ohnishi, and H. Ohno, Appl. Phys. Lett. **90**, 261112 (2007).
[41] J. Faist, F. Capasso, D. L. Sivco, A. L. Hutchinson, S. G. Chu, and A. Y. Cho, Appl. Phys. Lett. **72**, 680 (1998).
[42] J. Devenson, R. Teissier, O. Cathabard, and A. N. Baranov, Appl. Phys. Lett. **90**, 111118 (2007).
[43] H. M. Ng, C. Gmachl, S. N. G. Chu, and A. Y. Cho, J. Cryst. Growth **220**, 432 (2000).
[44] S. Nicolay, J. F. Carlin, E. Feltin, R. Butté, M. Mosca, N. Grandjean, M. Ilegems, M. Tchernycheva, L. Nevou, and F. H. Julien, Appl. Phys. Lett. **87**, 111106 (2005).
[45] X. Y. Liu, P. Holmström, P. Jänes, L. Thylén, and T. G. Andersson, Phys. Status Solidi B **244**, 2892 (2007).
[46] R. Q. Yang and S. S. Pei, J. Appl. Phys. **79**, 8197 (1996).

[47]R. Q. Yang, J. L. Bradshaw, J. D. Bruno, J. T. Pham, D. E. Wortman, and R. L. Tober, Appl. Phys. Lett. **81**, 397 (2002).
[48]T. J. Badcock, R. J. Royce, D. J. Mowbray, M. S. Skolnick, H. Y. Liu, M. Hopkinson, K. M. Groom, and Q. Jiang, Appl. Phys. Lett. **90**, 111102 (2007).
[49]S. Anantathanasarn, R. Nötzel, P. J. van Veldhoven, F. W. M. van Otten, Y. Barbarin, G. Servanton, T. de Vries, E. Smalbrugge, E. J. Geluk, T. J. Eijkemans, E. A. J. M. Bente, Y. S. Oei, M. K. Smit, and J. H. Wolter, Appl. Phys. Lett. **89**, 073115 (2006).
[50]G. Balakrishnan, S. H. Huang, T. J. Rotter, A. Stintz, L. R. Dawson, K. J. Malloy, H. Xu, and D. L. Huffaker, Appl. Phys. Lett. **84**, 2058 (2004); X. H. Tang, Z. Y. Yin, A. Y. Du, J. H. Zhao, and S. Deny, Trans. Nonferrous Met. Soc. China **16**, s25 (2006).
[51]V. Tasco, N. Deguffroy, A. N. Baranov, E. Tournié, B. Satpati, A. Trampert, M. S. Dunaevskii, and A. Titkov, Appl. Phys. Lett. **89**, 263118 (2006).
[52]C. Cornet, F. Doré, A. Ballestar, J. Even, N. Bertru, A. Le Corre, and S. Loualiche, J. Appl. Phys. **98**, 126105 (2005).
[53]F. Doré, C. Cornet, P. Caroff, A. Ballestar, J. Even, N. Bertru, O. Dehaese, I. Alghoraibi, H. Folliot, R. Piron, A. Le Corre, and S. Loualiche, Phys. Status Solidi C **3**, 3920 (2006).
[54]Y. Qiu, D. Uhl, and S. Keo, Appl. Phys. Lett. **84**, 263 (2004).
[55]J. P. Rosbeck, I. Kasai, R. M. Hoendervoogt, and M. Lanir, Tech. Dig. - Int. Electron Devices Meet. **1981**, pp. 161–164.
[56]E. Michel, J. Xu, J. D. Kim, I. Ferguson, and M. Razeghi, IEEE Photonics Technol. Lett. **8**, 673 (1996).
[57]M. Razeghi, Proc. SPIE **3629**, 2 (1999).
[58]L. O. Bubulac, A. M. Andrews, E. R. Gertner, and D. T. Cheung, Appl. Phys. Lett. **36**, 734 (1980).
[59]A. Rogalski, Prog. Quantum Electron. **27**, 59 (2003).
[60]Y. G. Zhang, Y. Gu, Ch. Zhu, G. Q. Hao, A. Zh. Li, and T. D. Liu, Infrared Phys. Technol. **47**, 257 (2006).
[61]J. H. Lee, S. S. Li, M. Z. Tidrow, and W. K. Liu, Infrared Phys. Technol. **42**, 123 (2001).
[62]S. V. Bandara, S. D. Gunapala, J. K. Liu, S. B. Rafol, C. J. Hill, D. Z. Ting, J. M. Mumolo, and T. Q. Trinh, Infrared Phys. Technol. **47**, 15 (2005).
[63]E. Luna, A. Guzmán, J. L. Sánchez-Rojas, E. Calleja, and E. Muñoz, Infrared Phys. Technol. **44**, 383 (2003).
[64]H. J. Haugan, G. J. Brown, F. Szmulowicz, L. Grazulis, W. C. Mitchel, S. Elhamri, and W. D. Mitchell, J. Cryst. Growth **278**, 198 (2005).
[65]A. Khoshakhlagh, J. B. Rodriguez, E. Plis, G. D. Bishop, Y. D. Sharma, H. S. Kim, L. R. Dawson, and S. Krishna, Appl. Phys. Lett. **91**, 263504 (2007); H. S. Kim, E. Plis, J. B. Rodriguez, G. D. Bishop, Y. D. Sharma, L. R. Dawson, S. Krishna, J. Bundas, R. Cook, D. Burrows, R. Dennis, K. Patnaude, A. Reisinger, and M. Sundaram, *ibid.* **92**, 183502 (2008).
[66]D. Pan, E. Towe, and S. Kennerly, Appl. Phys. Lett. **73**, 1937 (1998).
[67]H. Lim, S. Tsao, W. Zhang, and M. Razeghi, Appl. Phys. Lett. **90**, 131112 (2007).
[68]S. Tsao, H. Lim, W. Zhang, and M. Razeghi, Appl. Phys. Lett. **90**, 201109 (2007).
[69]S. Krishna, S. Raghavan, G. von Winckel, A. Stintz, G. Ariyawansa, S. G. Matsik, and A. G. U. Perera, Appl. Phys. Lett. **83**, 2745 (2003).